THE BORGNA-CONVERTER – A NEW TOPOLOGY FOR HIGHLY EFFICIENT PV INVERTERS

Luciano Borgna, Daniel Gfeller, Urs Muntwyler
Bern University of Applied Sciences (BFH), Laboratory for Photovoltaic Systems
Jlcoweg 1, CH-3400 Burgdorf, Switzerland, urs.muntwyler@bfh.ch, www.pvtest.ch

ABSTRACT: In this paper, a family of new and simple topologies for highly efficient, non-isolated switched-mode electronic power converters is introduced. Basically, these converters are quite similar to two-channel, interleaved buck-, boost- or buck-boost converters. However, the two sub-converters are connected with a small coupling capacitor in parallel to a small bypass switch. Also, the method of control of the power semiconductors is different. Due to these simple modifications, zero-current / zero-voltage switching is achieved, effectively reducing switching losses and electromagnetic interferences. With a prototype, the authors could show that more than 99% of efficiency can easily be achieved. However, compared to other soft-switching topologies, the complexity of these converters is low, and their method of control is simple. Even though the total number of power electronic components is higher compared to standard switched-mode power converters, the high efficiency and low electromagnetic interferences lead to reduced efforts for cooling and interference suppression, which compensates the costs of the power electronic components. This makes these new topologies ideally suited for cost-sensitive applications with high demands on efficiency such as photovoltaic inverters, power optimizers or battery storage systems. In addition to photovoltaic applications, there are several other areas in which these new converters can be used, such as electric cars or uninterruptable power supplies.
Keywords: Inverter, DC-DC-Converter, High-Efficiency

1 INTRODUCTION

Switched-mode power converters have found their way into many applications in both the industrial and domestic sector. Especially in the sectors of renewable energy and electrification of the road traffic, there are large and fast-growing markets for electronic power converters with both high demands on efficiency and high cost pressure [1, 2]. In the field of renewable energy, the solar inverter has proven to be a true technology driver in recent years. Where the peak efficiency of solar inverters in the nineties normally was below 95%, modern inverters have peak efficiency of more than 98%. Where an efficiency gain of 3% doesn't sound too spectacular, it must be considered that this also means a reduction of power losses by a factor of at least 2.5. This in turn means 2.5 times less heat dissipation and therefore considerably reduced cooling effort and lower thermal stressing of the components, resulting in potentially increased lifetime.

In a well-balanced switched-mode power converter, roughly 50% of the total power losses are dynamic losses caused by the limited switching speed of the power semiconductors. The other 50% are conduction losses caused by ohmic resistance in the current paths as well as core losses in the magnetic components. There are several approaches to reduce the power losses by elimination of the switching losses. Basically, this is achieved by zero-current switching (ZCS) or zero-voltage switching (ZVS) of the power semiconductors. These virtually lossless switching techniques can be found mainly in resonance converters. However, resonance converters are rather complex and require a sophisticated method of control. Because of this, resonance converters can only be found in some specialized applications and are virtually non-existent in cost-sensitive applications.

In this paper, a new family of topologies for non-isolated switched mode power converters is introduced. Even though the complexity of these converters is moderate, in combination with the right method of control, they effectively eliminate switching losses by use of zero-current and zero-voltage switching. As a result, an efficiency of more than 99% can be achieved (which has been proven with a prototype). Compared to the current market standard, the power losses of a PV inverter based on these new topologies will be only about half as high. This allows the design of compact devices with very low heat dissipation. A nice side-effect of the zero-current / zero-voltage switching is the elimination of hard switching edges, which effectively reduces the converter's electromagnetic interferences. Due to these benefits, the authors see great potential for this new technology not only in PV inverters, but also in many other applications such as battery charging systems, electric cars, uninterruptable power supplies and many more.

The converter topologies introduced in this paper have been invented by and named after Luciano Borgna, a long-time senior scientist at the Laboratory of Photovoltaic Systems of Bern University of Applied Sciences (BFH).

2 THEORY OF OPERATION

The Borgna-Converter's functional principle is explained on the basis of a unidirectional boost-converter. In the following explanation, we assume that the reader is familiar with the basic function of a boost-converter in discontinuous conduction mode and we will only investigate the specifics of a Borgna-Converter.

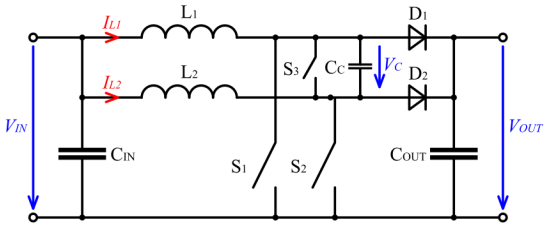

Figure 1: Topology of the Borgna-Boost-Converter (unidirectional)

The basic topology of the unidirectional Borgna-Boost-Converter is shown in Figure 1. The complete converter consists of two sub-converters in parallel operation. L_1, S_1 and D_1 form the first sub-converter. L_2, S_2 and D_2 form the second sub-converter. Furthermore, there are two additional components: A small coupling capacitor C_C and a small bypass switch S_3. In the following explanation, all components are assumed to be ideal. Moreover, C_{IN} and C_{OUT} are assumed to be large enough for the voltage ripple on both the input and the output to be neglected. In this example, the switches are symbolized by electromechanical contacts. In an actual design, they are of course replaced with suitable power semiconductors. One complete switching cycle consists of two half-cycles with a total of 14 steps. Steps 1 to 7 form the first half-cycle and steps 8 to 14 form the second half-cycle. Both half-cycles are almost identical, but with exchanged roles of the two sub-converters. The steps are explained below. In addition, Figure 2 visualizes the flow of current at the different steps of operation and Figure 3 shows the timing-diagram of the first half-cycle.

Step 1: Both sub-converters operate in discontinuous conduction mode. We will see later that during the zero-current phase, there is a small cross-current flowing through both inductors and the (at this time activated) bypass-switch S_3. The power switches S_1 and S_2 are turned on simultaneously at the beginning of step 1, which initializes the first half-cycle. Because of the discontinuous conduction mode, the activation of the switches occurs at zero-current (the cross-current does not flow through the power switches). After activation of the power switches, both inductor currents start to rise with a near-linear slope. S_3 is then turned off.

Step 2: Because of the initial cross-current, one of the inductors – in our example L_1 – carries a slightly higher current. Therefore, it will reach its desired peak-current a little earlier than L_2. As soon as the peak-value is reached, the first power switch S_1 is turned off. In a conventional design, this would cause a hard-switching slope. However, in the Borgna-Converter, the inductor current is redirected into the coupling capacitor. The charging of the coupling capacitor reduces the slew rate of the chopper voltage drastically. The resulting, low-gradient switching edge allows S_1 to turn-off at nearly zero-voltage. The switching energy is stored in the coupling capacitor.

Step 3: As soon as the voltage of the coupling capacitor reaches the output voltage, D_1 becomes conducting. The coupling capacitor remains charged to the converter's output voltage.

Step 4: Now, the second power switch S_2 is being turned off. Just like the first inductor's current in step 2, the second inductor's current I_{L2} is redirected into the coupling capacitor which is now discharged. This again leads to a low-gradient switching edge and allows S_2 to turn-off at nearly zero-voltage.

Step 5: As soon as the coupling capacitor is completely discharged, D_2 becomes conducting. Both inductors now transfer their energy into the output and the inductor currents fall back to zero. The coupling capacitor has now served its purpose and is bypassed by activation of the bypass switch S_3.

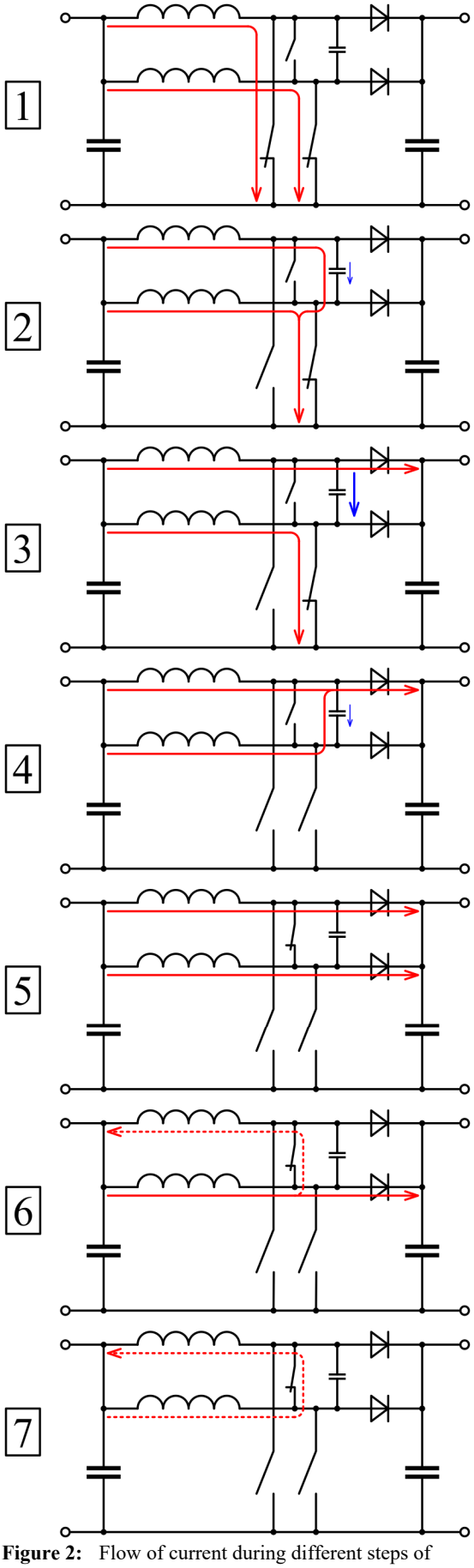

Figure 2: Flow of current during different steps of operation in the first half-cycle.

Step 6: As soon as the first inductor current I_{L1} crosses zero, D_1 starts to block. Now, an unwanted effect occurs. Because D_2 is still conducting, the first inductor is still negatively polarized, which leads the first inductor current to sink even further and to become slightly negative. However, the short-circuit switch S_3 prevents the coupling capacitor from unwanted charging.

Step 7: As soon as the second inductor current I_{L2} has the same absolute value as first inductor current I_{L1}, the current trough D_2 becomes zero and D_2 starts to block. The cross-current now flows in a loop between L_1, L_2 and S_3. This is virtually the same situation we had immediately prior to step 1, with the difference, that the cross-current now has inversed polarity. The first half-cycle is now complete, and the converter is ready for the next activation of the power switches.

Steps 8 to 14: The second half-cycle is almost identical to the first half-cycle. However, because the cross-current has changed its polarity, L_2 carries a slightly higher current than L_1 in step 8. Because of this, L_2 will reach the desired peak current first. Consequently, S_2 is turned-off first in the second half-cycle and as a result, the second inductor current I_{L2} will reach zero first. This again leads to a change of polarity of the cross-current. Thus, the situation at the end of step 14 is the same as it was immediately prior to step 1 and the cycle is complete.

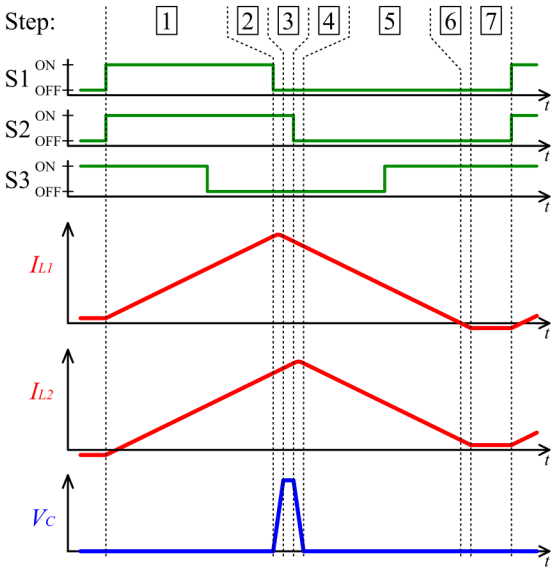

Figure 3: Timing-diagram of the first half-cycle.

Figure 3 shows the timing-diagram of the first half-cycle. It's plain to see that the first inductor current is always a little ahead of the second inductor current. The timing-diagram of the second half-cycle would look quite similar. However, in the second half-cycle, the second inductor current is a little ahead of the first inductor current, S_2 is turned off before S_1 and the coupling capacitor is charged with inversed polarity.

3 POSSIBLE EMBODIMENTS OF BORGNA-CONVERTERS

The differences between the Borgna-Boost-Converter and a standard interleaved boost-converter can be summarized as follows:

- Two sub-converters work in parallel mode like an interleaved converter. The only additional components are the coupling capacitor C_C and the bypass-switch S_3. These components connect the chopper-voltages of the two sub-converters.
- Both sub-converters operate in discontinuous conduction mode. This allow the power switches to be turned on at zero-current. At the begin of a switching cycle, both power switches are turned on simultaneously.
- The power switches are turned off with a time delay. This allows the corresponding inductor current to be redirected into the coupling capacitor. The charging or discharging of the coupling capacitor reduces the voltage gradient of the chopper voltage and allows the power switches to be turned off at nearly zero-voltage.
- The bypass-switch prevents the coupling-capacitor from unwanted charging by the cross-current during the zero-current phase.

These modifications can also be applied to both the buck- and the buck-boost-converter. The unidirectional topologies of the Borgna-Buck-Converter and the Borgna-Buck-Boost-Converter are shown in Figure 4.

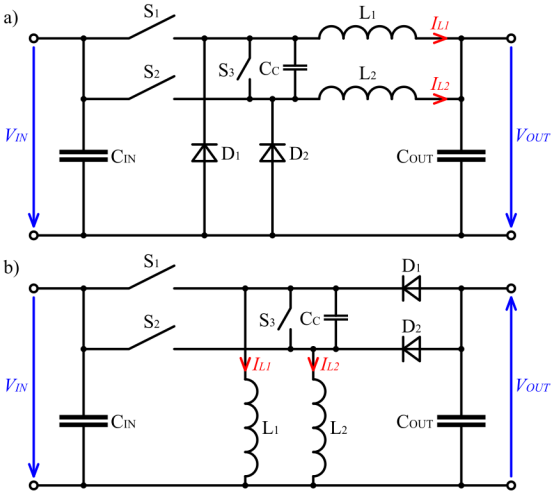

Figure 4: Unidirectional Borgna-Converter topologies:
a. Borgna-Buck-Converter
b. Borgna-Buck-Boost-Converter

With the common dc-to-dc converter topologies, bidirectional operation becomes possible by replacing the diode with additional switches. This is also possible with Borgna-Converters. Figure 5 shows the bidirectional embodiments of the Borgna-Buck-Converter and the Borgna-Buck-Boost-Converter. Not shown is the bidirectional Borgna-Boost-Converter, which is simply a Borgna-Buck-Converter (as shown in Figure 5a) with power flow from right to left. Needless to say, with bidirectional topologies, the switches must be handled with special care, because an on-state of both switches of the same sub-converter at the same time leads to a short circuit and most probably to the destruction of the

converter. Additionally, with bidirectional Borgna-Converters, the switches replacing the diodes should be activated at the exact very moment, when the voltage over the switches crosses zero.

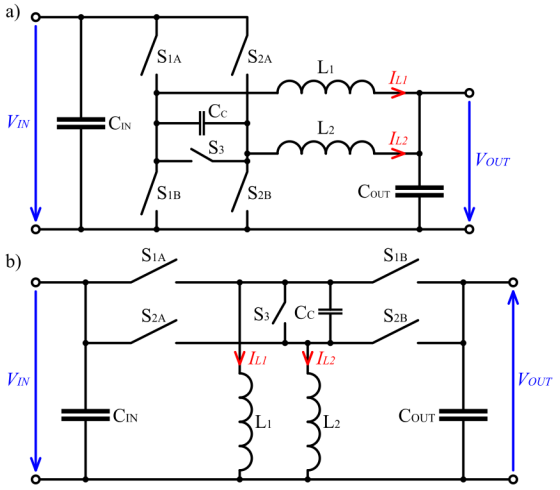

Figure 5: Bidirectional Borgna-Converter topologies:
a. Borgna-Buck-Converter
b. Borgna-Buck-Boost-Converter

This is not trivial, because this moment depends on the charging time of the coupling capacitor, which in turn depends on the charging current (which is basically the peak inductor current). However, this problem can easily be avoided by adding a diode in parallel to the switch, which automatically becomes conducting at the right time (just as it does in the unidirectional topologies). Fortunately, in most cases, the required diodes are already present in form of the body diodes of the power switches. If there are diodes in parallel to the switches, depending on the direction of the flow of power, the corresponding switches don't necessarily have to be activated at all. Figure 6 shows this on the example of the bidirectional Borgna-Buck-Converter. If the power flows from left to right, the converter operates in buck-mode. In this mode, only the high-side switches need to be driven.

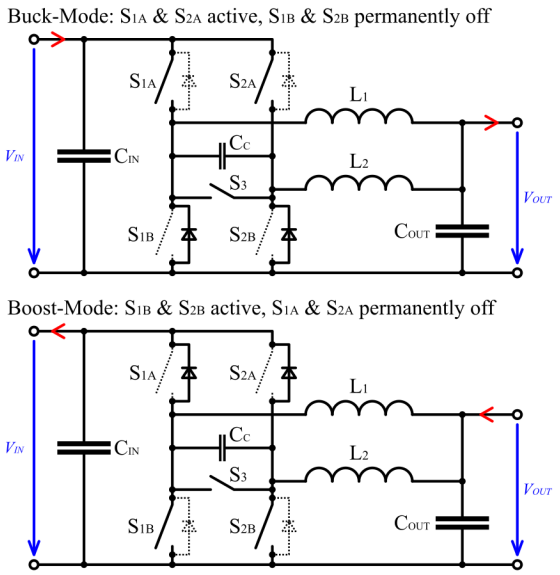

Figure 6: Active power electronic components during buck- and buck-boost-mode

The low-side switches can be turned off permanently as only their (body-) diodes are needed. The circuit is then identical to the unidirectional Borgna-Buck-Converter as shown in Figure 4a. If the power flows from right to left, the converter operates in boost-mode. In this mode, only the low-side switches need to be driven and the high-side switches work as diodes. If we flip this circuit horizontally, it becomes identical to the unidirectional Borgna-Boost-Converter as shown in Figure 1. In some cases, it will still be useful to drive the additional two switches, regardless in which mode the converter operates. This is the case if the voltage drop of the diode is higher than the voltage drop of the corresponding switch in on-state. The activation of the switch will then minimize the conduction losses, but it is essential that the switch is only turned on when the diode is forward biased.

So far, we only discussed DC-to-DC converters. However, by modulation of the output voltage, AC waveforms can be generated as well. As an example, three bidirectional Borgna-Buck-Converters can be combined to a full three-phase inverter (Figure 7). In general, the Borgna-Converter's basic principle is applicable to most inverter topologies (such as H4, H5, H6 or HERIC).

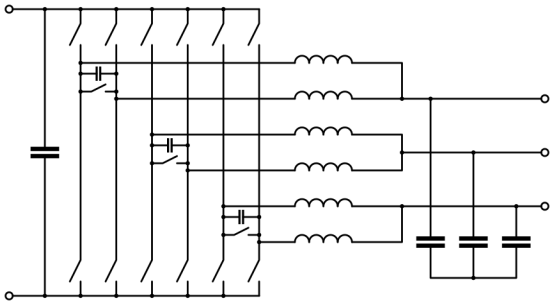

Figure 7: Three-phase Borgna-Inverter topology

4 EXPERIENCES WITH A PROTOTYPE

As proof of concept, the authors have designed, assembled and tested a prototype of a bidirectional Borgna-Buck-Converter. The PCB of the prototype's power stage is shown in Figure 8. Table I gives an overview of the prototype's nominal technical data. Figure 9 shows the simplified schematic of the prototype's power stage and Table II lists the power components used.

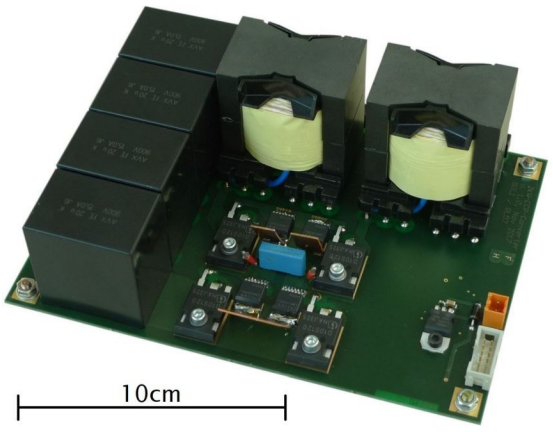

Figure 8: Prototype Borgna-Converter

Table I: Outline of nominal technical data

	Symbol	Value
input voltage	V_{IN}	800 V
input current	I_{IN}	2.5 A
output voltage	V_{OUT}	400 V
output current	I_{OUT}	5 A
output power	P_{OUT}	2 kW
switching frequency	f_{SW}	50 kHz

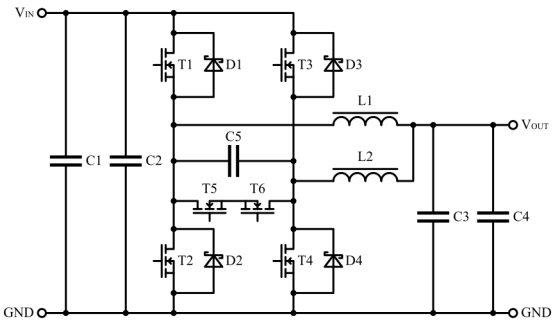

Figure 9: Simplified schematic of the prototype Borgna-Converter

Table II: Bill of materials

Pos.	Manufacturer Type	Description
C1-C4	AVX FE37M6C0206KB	film capacitor 20 µF / 900 V
C5	TDK / EPCOS B32682A2102K000	film capacitor 1 nF / 2000 V
D1-D4	Infineon IDW10S120	SiC Schottky Diode 10 A / 1200 V
L1, L2	Self-wound inductor, L ≈ 648µH, core PQ 50/50, core material N95, air gap ca. 4.3mm, 84 turns of high-frequency stranded wire (270 x 0.004 mm²)	
T1-T4	Wolfspeed C3M0120090J	SiC MOSFET 900 V / 22 A / 120 mΩ
T5, T6	Wolfspeed C3M0280090J	SiC MOSFET 900 V / 11 A / 280 mΩ

A few remarks on the prototype and the choice of components:

- The prototype is a demonstrator, designed according to the best practice method. It is supposed to show what's possible with a Borgna-Converter. Therefore, the components have been chosen solely about technical and not economical aspects. Because of this, SiC MOSFETs and diodes haven been chosen. They are rather expensive, but represent the latest state of the art.

- In buck-mode, T1 and T3 are active. In boost-mode, T2 and T4 are active. It would be possible to turn-on the other two transistors during the demagnetization phase of the inductors to take some of the current from the diodes. With this, the conduction losses could virtually be reduced by half. As this is not without risk, it was not implemented in the prototype.

- T5 and T6 form the short-circuit switch. As they should carry the cross-current only (about 620mA during the zero-current phase), they are oversized.

- The control unit for the prototype was implemented with an 8-bit microcontroller type ATmega16 from Atmel. The controller generates a pulse with modulated signal with fixed frequency and variable pulse width. The control unit has deliberately been kept simple and is not optimized for speed. Its sole purpose is to provide a stable operating point so that measurements on the prototype can be performed easily.

- Originally, ultralow ESR electrolytic capacitors should have been used on both input and output. However, our investigation showed that high-capacity foil capacitors (also known as dc link capacitors) are a better option. Due to their low ESR (5.5 mΩ) and high resonance frequency (nearly 200 kHz), two such foil capacitors of 20 µF in parallel provide a better ripple rejection than one single ultralow ESR electrolytic capacitor of 820 µF. Moreover, they can withstand higher ripple currents, have a considerable higher lifetime and cost less.

4.1 Efficiency of the power conversion

The prototype's efficiency has been measured with a precision power analyzer type WT3000 from Yokogawa. Figure 10 shows the efficiency in both buck- and boost-mode as a function of the output power. It must be remarked that the measurement does not include the power consumption of the control unit and the MOSFET drivers. However, these add up to less than 600 mW, which is less than 0.03% of the prototype's rated power (and the control unit hasn't even been optimized for low power). The peak efficiency in both modes is about 99.4% at 1500 W output power. Especially for a converter of this size, this is a very good value. However, it's plain to see that the efficiency curves have a distinct ripple. For example, between 1200 W and 1500 W, the efficiency rises about 1% (which, in relation to the high peak efficiency, is a lot).

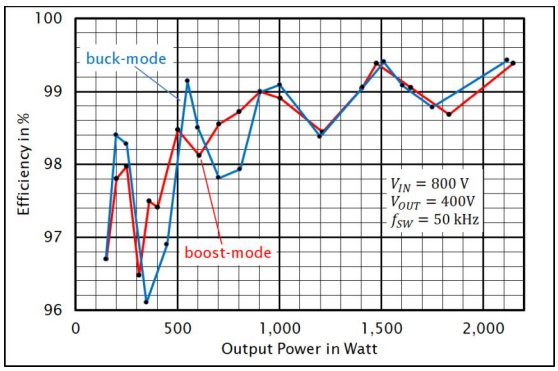

Figure 10: Efficiency of the prototype in buck- and boost-mode

The unstable efficiency is caused by an unwanted oscillation effect during the zero-current phase of the converter (also known as inductor current ringing). When all power electronic components (MOSFETs and diodes) are blocking, the inductors form a series resonance with the parasitic capacitance of the common node of the inductors and MOSFETs. This parasitic capacitance

equals to a few 100pF and is mainly caused by the MOSFET's output capacitance. If the MOSFETs are turned on at the end of the zero-current phase, this capacitance is shorted, and the energy stored inside the capacitance is being dissipated in the MOSFETs. Depending on the instantaneous value of the capacitance's voltage at the end of the zero-current phase, this leads to a certain power loss. As this instantaneous value depends on the duration of the zero-current phase, it also depends on the duty-cycle of the pulse width modulation and therefore depends on the output power. In an optimized design, the zero-current phase must have the right duration, so that the turn-on of the MOSFETs occurs exactly at the very moment, when the voltage of the parasitic capacitance has its minimum value (ideally zero). If the design is optimized in this way, the use of SiC MOSFETs is no longer mandatory to achieve high performance (with the prototype, the SiC MOSFETs have mainly been evaluated because of their low output capacitance). Due to zero-voltage switching, there is not even a need for fast-switching semiconductors. It should also be mentioned, that the oscillation effect during the zero-current phase is not only present in Borgna-Converters, but in all converters operating in discontinuous conduction mode [3]. However, with conventional converters, the efficiency is usually much lower, making the effect far less noticeable.

4.2 Electromagnetic compatibility

The electromagnetic disturbances have been measured according to CISPR 11 (conducted emissions). With a quasi-peak measurement in the normative frequency range of 150kHz to 30MHz, the conducted emissions were below 80 dBµV on all terminals. It must be emphasized that this value has been achieved without any measures for EMC suppression. If the device is simply put into a metal casing to shield capacitive coupling to the environment and small chokes of 1 µH are applied in series to both input and output, the emissions fall below 70 dBµV and with that well below the normative limits for class B devices. For a converter of 2 kW without any filtering, this is a more than respectable result. With both, the very high peak efficiency and the excellent EMC behavior, the prototype has proven that with the Borgna-Converter, a superior performance can be achieved. However, as we will see in the next section, there is still some room for improvement.

4.3 Further optimization of the prototype

The largest potential for improvement lies in the instability of the efficiency as shown in Figure 10. We already mentioned, that the ideal situation was if the MOSFETs would be turned on at the very moment when their parasitic output capacitance is at zero-voltage. Therefore, the key to optimal performance lies in the right method of control. The authors assume that with an optimized controller, the prototype will achieve a stable efficiency of >99% between 25% and 110% of its nominal power. There are several ways that lead to this goal [4]. The straightforward approach would be to measure the voltage and let the control unit process this data. However, such a sophisticated measurement might get in conflict with the cost-sensitivity. A low-cost approach would be to calculate the optimal duration of the zero-current phase as a function of the oscillation frequency. Unfortunately, the oscillation frequency is not stable because the parasitic capacitance is not constant (the MOSFET's output capacitance is highly voltage-sensitive and subject to specimen scattering). But this can easily be solved, by adding an additional capacitor between the chopper voltage and ground, i.e. in parallel to the parasitic capacitance. The capacitance of this capacitor shall be large compared to the parasitic capacitance, with the aim to make the oscillation frequency more deterministic (the influence of the parasitic capacitance then becomes negligible). Of course, with this method, it is imperative that the turn-on of the MOSFETs happens exactly when the capacitor is at zero-voltage. Otherwise, the energy stored in the additional capacitor will be dissipated which as well would increase the total losses considerably. Also, as there is no power transfer during the zero-current phase of the inductors, this phase should be kept as short as possible. Consequently, the time of steps 7 or 14 should be half a period of the parasitic oscillation (at the begin of steps 7 and 14, the voltage of the parasitic capacitance's voltage is at maximum, therefore it will be at minimum one half-wave later). A control unit with the ability to achieve this, must be able to generate a PWM signal with modulation of both pulse width and frequency. As a next step, the authors intend to upgrade the prototype with such a control unit. In the same turn, the control unit shall be configured to also turn-on the MOSFETs in parallel to the diodes when the diodes are conducting. Due to the reduction of conduction losses, the authors assume an efficiency gain of roughly 0.1%. Moreover, a preliminary test has shown, that the prototype has an even better performance in buck-mode with 600 V input and 400 V output voltage. If only the power electronic components for this mode are being assembled (removing of D1, D3, T2 & T4 in Figure 8), a peak efficiency of even 99.6% has been measured.

5 CONCLUSIONS

With the results of the prototype, the authors could show that the Borgna-Converter does have a superior performance compared to standard, hard-switching DC-to-DC-converters. With both, the high efficiency and the very good EMC behavior, the prototype has exceeded the author's expectations. With the modifications presented, an even better performance can be assumed. The impact of this new technology to the market will depend on how cost-effective the Borgna-Converter can be implemented. There are some rivalling factors. On one side, there are the costs of power electronic components and inductors. As a Borgna-Converter always consists of two sub-converters, compared to standard DC-to-DC-converters, these costs are higher. On the other side, because of the superior performance, considerable savings of costs for both cooling and EMC suppression can be assumed. This might already lead to competitive manufacturing costs in some cases. However, if the savings in energy costs due to the high efficiency are also being considered, the total lifetime costs will be significantly lower in many cases. For reasons of scalability, large converters sometimes already have a modular design with several sub-converters in parallel operation. If this is the case, then there is little reason not to couple the sub-converters into pairs and let them work as Borgna-Converters – the additional costs are minimal. In summer 2018, a patent application has been filed for the Borgna-Converter. The

authors are now looking for partners, which are interested to use this new converter technology.

6 ACKNOWLEDGMENTS

This research is part of the activities of the Swiss Centre for Competence in Energy Research on the Future Swiss Electrical Infrastructure (SCCER-FURIES), which is financially supported by the Swiss Innovation Agency (Innosuisse - SCCER program). We also gratefully acknowledge funding from Bern University of Applied Sciences BFH, Burgdorf, Switzerland.

7 REFERENCES

[1] Schmela Michael et al.: Global Market Outlook for Solar Power 2019-2023, SolarPower Europe (SPE, formerly known as EPIA) Press Release (www.solarpowereurope.org)

[2] Turk Dave et al.: Global EV Outlook 2018, International Energy Agency (IEA) Publications (www.iea.org)

[3] Walczac Marcin: Impact of Inductor Current Ringing in DCM on output Voltage of DC-DC Buck Power Converters, Archives of Electrical Engineering Vol 66 pp. 313-323

[4] Hoi Lee, Seong-Ryong Ryu: An Efficiency-Enhanced DCM Buck Regulator with Improved Switching Timing of Power Transistors, IEEE Transactions on Circuits and Systems II: Express Briefs Vol. 57, March 2010